Applied and Computational Mechanics 6 (2012) 151–162

Modeling of damage evaluation in thin composite plate loaded by pressure loading

M. Dudinský[a,*], M. Žmindák[a], P. Frnka[a]

[a] *Faculty of Mechanical Engineering, University of Žilina, Univerzitná 1, 010 26 Žilina, Slovak Republic*

Received 5 July 2012; received in revised form 7 December 2012

Abstract

This article presents the results of numerical analysis of elastic damage of thin laminated long fiber-reinforced composite plate consisting of unidirectional layers which is loaded by uniformly distributed pressure. The analysis has been performed by means of the finite element method (FEM). The numerical implementation uses layered plate finite elements based on the Kirchhoff plate theory. System of nonlinear equations has been solved by means of the Newton-Raphson procedure. Evolution of damage has been solved using the return-mapping algorithm based on the continuum damage mechanics (CDM). The analysis was performed using own program created in MATLAB. Problem of laminated fiber-reinforced composite plate fixed on edges for two different materials and three different laminate stacking sequences (LSS) was simulated. Evolution of stresses vs. strains and also evolution of damage variables in critical points of the structure are shown.

Keywords: damage, finite element method, continuum damage mechanics, composite plate

1. Introduction

Composite materials are now common engineering materials used in a wide range of applications. They play an important role in the aviation, aerospace and automotive industry, and are also used in the construction of ships, submarines, nuclear and chemical facilities, etc. The meaning of the word damage is quite broad in everyday life. In continuum mechanics the term damage is referred to as the reduction of the internal integrity of material due to generating, spreading and merging of small cracks, cavities and similar defects. In the initial stages of the deformation process the defects (microcracks, microcavities) are very small and relatively uniformly distributed in the microstructure of a material. If the damage reaches the critical level (depends on type of loading and used material), subsequent growth of defects will concentrate in some of the defects already present in material [7]. Damage is called elastic, if the material deforms only elastically (in macroscopic level) before the occurrence of damage, as well as during its evolution. This damage model can be used if the ability of the material to deform plastically is low. Fiber-reinforced polymer matrix composites can be considered as such materials [11]. Commercial FEM software can perform analyses with many types of material nonlinearities, such as plasticity, hyperelasticity, viscoplasticity, etc. However, almost no commercial software (except for ABAQUS) contains a module for damage analysis of composite materials.

The goal of this paper is to present the numerical results of elastic damage analysis of thin laminated composite plate consisting of unidirectional long fiber-reinforced layers which is

*Corresponding author. Tel.: +421 415 132 974, e-mail: martin.dudinsky@fstroj.uniza.sk.

loaded by uniformly distributed pressure. The analysis was performed by own software created in MATLAB programming language. This software can perform numerical analysis of elastic damage based on continuum damage mechanics utilizing finite element method using layered plate finite elements based on the Kirchhoff plate theory. Locking effect was not removed, since this is a rather complicated issue.

2. Theoretical and numerical modeling background

A number of material modeling strategies exist to predict failure in laminated composites, subjected to static or impulsive loads. Broadly, they can be classified as [12, 15, 19]:

- strength-based failure criteria,
- fracture mechanics approach (based on energy release rates),
- plasticity or yield surface approach,
- damage mechanics approach.

Strength-based failure criteria (failure criteria approach) are commonly used with FEM to predict failure events in composite structures. These approaches are based on the equivalent stresses or strains in the critical failure areas. Numerous criteria have been derived to relate internal stresses and experimental measures of material strength to the onset of failure (maximum stress or strain, Hill, Hoffman, Tsai-Wu, etc.). These classical criteria implemented in most commercial FE codes are not able to physically capture the failure mode. Some of them cannot deal with materials having a different strength in tension and compression. The Hashin criteria are briefly reviewed in [11] and improvements were proposed by Puck and Schurmann [14] over Hashin's theories are examined.

However, few criteria can represent several relevant aspects of the failure process of laminated composites, e.g. the increase on apparent shear strength when applying moderate values of transverse compression, or detrimental effect of the in-plane shear stresses in failure by fiber kinking.

2.1. Continuum damage mechanics

From a physical point of view, damage represents surface discontinuities in form of microcracks or volume discontinuities in form of cavities in a material. They are formed as the material undergoes an increasing loading. The objective of the damage mechanics is to predict, through mechanical variables, the response of a material in the presence of damage. Damage is initiated at certain stress level and it generally increases with increasing stress from the virgin state up to a macroscopic crack initiation or failure.

Continuum Damage Mechanics (CDM) considers damaged materials as a continuum, in spite of heterogenity, micro-cavities, and micro-defects. The response to the loading conditions is determined on the basis of the constitutive relations between macroscopic variables (e.g. stress, strain) and internal variables which model, on a macroscopic scale, the irreversible changes occurring at the microscopic level.

We consider a volume of material free of damage if no cracks or cavities can be observed at the microscopic scale. The opposite state is the fracture of the volume element. Theory of damage describes the phenomena between the virgin state of material and the macroscopic

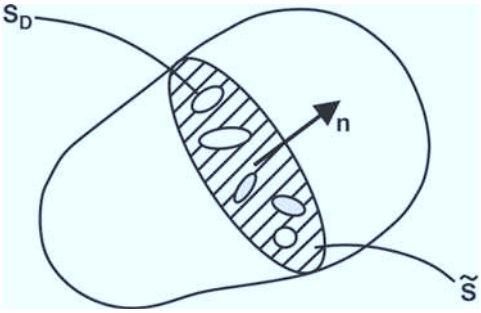

Fig. 1. Representative volume element for damage mechanics

onset of crack [6, 16]. The representative volume element must be of sufficiently large size compared to the inhomogenities of the composite material. In Fig. 1 this volume is depicted. One section of this element is related to its normal and to its area S. Due to the presence of defects, an effective area $\tilde{S}$ for resistance of load can be found. Total area of defects is therefore

$$S_D = S - \tilde{S}. \tag{1}$$

The local damage related to the direction $\mathbf{n}$ is defined as:

$$D = \frac{S_D}{S}. \tag{2}$$

For isotropic damage, the dependence on the normal $\mathbf{n}$ can be neglected, i.e.

$$D = D_n \, \forall n. \tag{3}$$

We note that damage D is a scalar assuming values between 0 and 1. For $D = 0$ a material is undamaged, for $0 < D < 1$ a material is damaged, for $D = 1$ complete failure occurs. The quantitative evaluation of damage is not a trivial issue, it must be linked to a variable that is able to characterize the phenomenon. Several papers can be found in literature where the constitutive equations of the materials are a function of a scalar variable of damage [2, 3]. For the formulation of a general multidimensional damage model it is necessary to generalize the scalar damage variables. It is therefore necessary to define corresponding tensorial damage variables that can be used for general states of deformation and damage [18].

2.2. Numerical modeling

One of the most powerful computational methods for structural analysis of composites is the FEM. The starting point should be a "validated" FE model, with a reasonably fine mesh, correct boundary conditions, material properties, etc. [1]. As a minimum requirement, the model is expected to produce stress and strains that have reasonable accuracy to those of the real structure prior to failure initiation. In spite of a great success of the finite and boundary element methods as effective numerical tools for the solution of boundary-value problems on complex domains, there is still growing interest in the development of new advanced methods. Many meshless formulations are becoming popular due to their high adaptivity and a low cost to prepare input data for numerical analysis [4, 5, 13].

2.3. FEM formulation for Kirchhoff plate

Plate models are used to study structural components which are subjected to bending loads and their thickness is smaller than the others dimensions. This characteristic allows representing the plate using the reference middle surface. Therefore the geometric domain used for the formulation of plate models is the middle surface.

A plate resists transverse loads by means of bending, exclusively. The flexural properties of a plate depend greatly upon its thickness in comparison with other dimensions. Plates may be classified into three groups according to the ratio a/t, where a is a typical dimension of a plate in a plane and t is a plate thickness. The first group is represented by thick plates having ratios $a/t \leq 8 \ldots 10$. The second group refers to plates with ratios $a/t \geq 80 \ldots 100$. These plates are referred to as membranes. The most extensive group represents an intermediate type of plates, so-called thin plates with $8 \ldots 10 \leq a/t \leq 80 \ldots 100$ [17].

One of the most widely used theory for thin plates is the Kirchhoff (classical) plate theory. The Kirchhoff (classical) laminate plate theory and the first-order shear deformation theories describe with reasonable accuracy the kinematics of most laminates [19]. The details of derivation of equations governing the behavior of thin plates are given in [17]. The equations are represented here for clarity.

In this subsection formulation for plate element based on the Kirchhoff plate theory for symmetric balanced laminate will be presented. The most widely used plate elements in FEM are linear and quadratic elements with 3 degrees of freedom (DOFs) in node: w, θ_x, θ_y. When using linear four-node elements, one element has 12 DOFs and 12 shape functions are required.

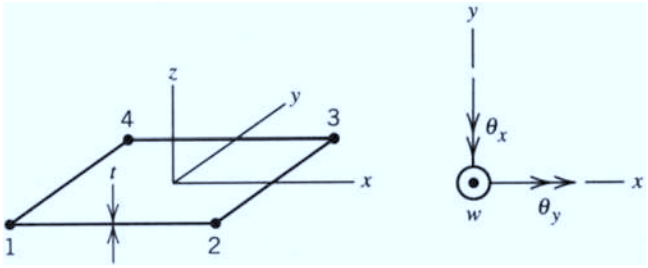

Fig. 2. Four-node Kirchhoff plate element and DOFs in node

It is worth noting that shape functions must have C^1 continuity. Displacements within the element are interpolated as

$$w = \mathbf{N}\,\hat{\mathbf{u}} \tag{4}$$

where w is displacement in given point of the element, $\mathbf{N} = [N_1, N_2, \ldots, N_{3xn}]$ is vector of values of shape functions in this point, n is number of nodes in element and $\hat{\mathbf{u}} = \left[\hat{w}_1, \hat{\theta}_{x1}, \hat{\theta}_{y1}, \ldots, \hat{w}_n, \hat{\theta}_{xn}, \hat{\theta}_{yn}\right]^T$ is vector of nodal displacements.

Matrix $\mathbf{B}$, which in the case of plate elements gives the relation between curvatures and nodal displacements, has the form of

$$\mathbf{B} = \begin{bmatrix} \dfrac{\partial^2 N_1}{\partial x^2} & \dfrac{\partial^2 N_2}{\partial x^2} & & \dfrac{\partial^2 N_n}{\partial x^2} \\ \dfrac{\partial^2 N_1}{\partial y^2} & \dfrac{\partial^2 N_2}{\partial y^2} & \cdots & \dfrac{\partial^2 N_n}{\partial y^2} \\ 2\dfrac{\partial^2 N_1}{\partial x \partial y} & 2\dfrac{\partial^2 N_2}{\partial x \partial y} & & 2\dfrac{\partial^2 N_n}{\partial x \partial y} \end{bmatrix}. \tag{5}$$

The element stiffness matrix for unidirectional element has the form of

$$\mathbf{k} = \int_A \mathbf{B}^T \mathbf{D_K} \mathbf{B} \, \mathrm{d}A. \tag{6}$$

Matrix $\mathbf{D_K}$ gives the relation between internal moments and curvatures. More details about this matrix are given e.g. in [9]. The element stiffness matrix is integrated numerically, most often by means of Gauss quadrature [10]. The element stiffness matrix calculation for layered rectangular element with edges parallel to x and y axis by means of Gauss quadrature is performed as follows

$$\begin{aligned} \mathbf{k} &= \sum_{n=1}^{NL} \int_{x_1}^{x_2} \int_{y_1}^{y_4} \mathbf{B}^T \mathbf{D_K} \mathbf{B} \, \mathrm{d}y \, \mathrm{d}x \approx \\ &\approx \sum_{n=1}^{NL} \sum_{i=1}^{n_{Gx}} \frac{x_2 - x_1}{2} \sum_{j=1}^{n_{Gy}} \frac{y_4 - y_1}{2} \mathbf{B}^T(x_{int_i}, y_{int_j}) \mathbf{D_K} \mathbf{B}(x_{int_i}, y_{int_j}) W_i W_j, \end{aligned} \tag{7}$$

$$x_{int_i} = \frac{x_2 - x_1}{2} x_{Gi} + \frac{x_2 + x_1}{2}, \tag{8}$$

$$y_{int_j} = \frac{y_4 - y_1}{2} y_{Gj} + \frac{y_4 + y_1}{2}, \tag{9}$$

where NL is number of layers, x_1, x_2, y_1, y_4 are x and y coordinates of nodes, which are in subscript, x_{Gi}, y_{Gj} are Gauss points, W_i, W_j are corresponding weights and n_{Gx} and n_{Gy} is number of Gauss points in x- and y-axis direction.

3. Damage model used

The model for fiber-reinforced lamina mentioned next was presented by Barbero and de Vivo [2] and is suitable for fiber-reinforced composite materials with polymer matrix. On the lamina level these composites are considered as ideal homogenous and transversely isotropic. All parameters of this model can be easily identified from available experimental data. It is assumed that damage in principal directions is identical with the principal material directions (1, 2, 3) throughout the damage process. This is due to the fact that the dominant modes of damage are micro-cracks, fiber breaks and fiber-matrix debond, all of which can be conceptualized as cracks parallel or perpendicular to the fiber direction [3]. Therefore the evolution of damage is solved in the lamina coordinate system. The model predicts the evolution of damage and its effect on stiffness and subsequent redistribution of stress.

3.1. Damage surface and damage potential

Damage surface is defined by tensors $\mathbf{J}$ and $\mathbf{H}$ [3]

$$J = \begin{bmatrix} J_{11} & 0 & 0 \\ 0 & J_{22} & 0 \\ 0 & 0 & J_{33} \end{bmatrix}, \qquad H = [H_1, H_2, H_3]. \tag{10}$$

Damage surface is similar to the Tsai-Wu damage surface [6], and it is commonly used for predicting failure of fiber-reinforced lamina with respect to experimental material strength

values. Damage surface and damage potential have the form of [3]

$$g(\mathbf{Y},\gamma) = \sqrt{J_{11}Y_1^2 + J_{22}Y_2^2 + J_{33}Y_3^2} + \sqrt{H_1Y_1^2 + H_2Y_2^2 + H_3Y_3^2} - (\gamma + \gamma_0), \quad (11)$$

$$f(\mathbf{Y},\gamma) = \sqrt{J_{11}Y_1^2 + J_{22}Y_2^2 + J_{33}Y_3^2} - (\gamma + \gamma_0), \quad (12)$$

where the thermodynamic forces Y_1, Y_2 and Y_3 can be calculated by means of relations

$$\begin{aligned} Y_1 &= \frac{1}{\Omega_1^2}\left(\frac{\bar{S}_{11}}{\Omega_1^4}\sigma_1^2 + \frac{\bar{S}_{12}}{\Omega_1^2\Omega_2^2}\sigma_1\sigma_2 + \frac{\bar{S}_{66}}{\Omega_1^2\Omega_2^2}\sigma_6^2\right), \\ Y_2 &= \frac{1}{\Omega_2^2}\left(\frac{\bar{S}_{22}}{\Omega_2^4}\sigma_2^2 + \frac{\bar{S}_{12}}{\Omega_1^2\Omega_2^2}\sigma_1\sigma_2 + \frac{\bar{S}_{66}}{\Omega_1^2\Omega_2^2}\sigma_6^2\right), \\ Y_3 &= 0. \end{aligned} \quad (13)$$

where stresses and components of matrix $\bar{S}$ are defined in the lamina coordinate system. Matrix $\bar{S}$ gives the strain-stress relations in the effective configuration [2]. Ω_1 and Ω_2 are components of a second-order tensor $\mathbf{\Omega} = \sqrt{\mathbf{I} - \mathbf{D}}$, called the integrity tensor. The eigenvalues D_i of damage tensor $\mathbf{D}$ describe the load-carrying area reduction on the three planes orthogonal to the principal direction of the tensor $\mathbf{D}$. Equations (11) and (12) can be written for particular simple stress states: tension and compression in fiber direction, tension in transverse direction, in-plane shear. Tensors $\mathbf{J}$ and $\mathbf{H}$ can be derived in terms of material strength values.

3.2. Hardening parameters

In the present damage model isotropic hardening is considered and hardening function was used in the form of

$$\gamma = c_1\left[\exp\left(\frac{\delta}{c_2}\right) + 1\right]. \quad (14)$$

where δ denotes the hardening variable. The hardening parameters γ_0, c_1 and c_2 are determined by approximating the experimental stress-strain curves for in-plane shear loading. If this curve is not available, we can reconstruct it using the function

$$\sigma_6 = F_6 \tanh\left(\frac{G_{12}}{F_6}\gamma_6\right), \quad (15)$$

where F_6 is the in-plane shear strength, G_{12} is the in-plane initial (undamaged) shear modulus and γ_6 is the in-plane shear strain (in the lamina coordinate system). This function represents experimental data very well.

3.3. Critical damage level

Reaching of critical damage level is dependent on stress values in lamina. If in a point in lamina only normal stresses in the fiber direction and across the fibers (i.e. normal stresses in lamina coordinate system) occur, then simply comparing the values of damage variables with critical values of damage variables for given material at this point is sufficient. The damage has reached the critical level if at least one of the values of D_1, D_2 in the point of lamina is greater or equal to its critical value. The magnitude of these critical damage parameter values can be estimated from statistical models of the failure process of each type of loading. If in given point of lamina also shear stress occurs (in lamina coordinate system), it is additionally necessary to compare

the value of the product of $(1 - D_1)(1 - D_2)$ with value of k_s parameter from Table 3 for given material. If the value of this product is less or equal to k_s, the damage has reached the critical level. Value of k_s is determined from the relation between damaged in-plane shear modulus G_{12}^* and undamaged in-plane shear modulus G_{12}

$$k_s = \frac{G_{12}^*}{G_{12}}. \tag{16}$$

3.4. Implementation of numerical method

The Newton-Raphson method was used for solving the system of nonlinear equations. Evolution of damage has been solved using the return-mapping algorithm described in [2]. The input values are strains and strain increments in lamina coordinate system, state variables D_1, D_2, and δ in integration point from the start of the last performed iteration, $\bar{\mathbf{C}}$ matrix (gives the stress-strain relations in the effective configuration [3]) and damage parameters related to damage model. The output variables are D_1, D_2, and δ, stresses and strains in lamina coordinate system in this integration point at the end of the last performed iteration. Another output is damaged tangent constitutive matrix $\mathbf{C}^{\mathbf{ed}}$ in lamina coordinate system, which reflects the effect of damage on the behavior of structure. Flowchart of the return-mapping algorithm used in numerical damage analysis is described in Fig. 3.

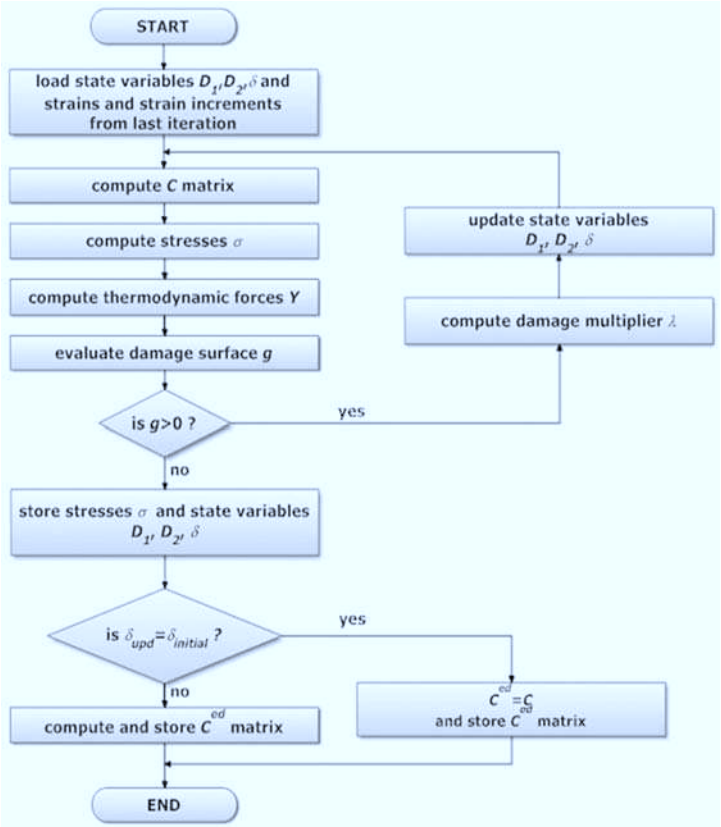

Fig. 3. Flowchart of the return-mapping algorithm used in numerical damage analysis of thin composite plates

4. Numerical example and results

One problem for two different materials and three different laminate stacking sequences (LSS) was simulated in order to study damage of laminated long fiber-reinforced composite plates consisting of unidirectional layers. Composites consist of carbon fibers embedded in epoxy matrix. Composite plate fixed on its edges with dimensions of $125 \times 125 \times 2.5$ mm and LSS of $[0, 45, -45, 90]_S$, $[0, 90, 45, -45]_S$ and $[45, 0, -45, 90]_S$ was loaded by uniformly distributed pressure $p = 0.5$ MPa perpendicular to the surface of the plate (Fig. 4). Own program created in MATLAB language was used for this analyses.

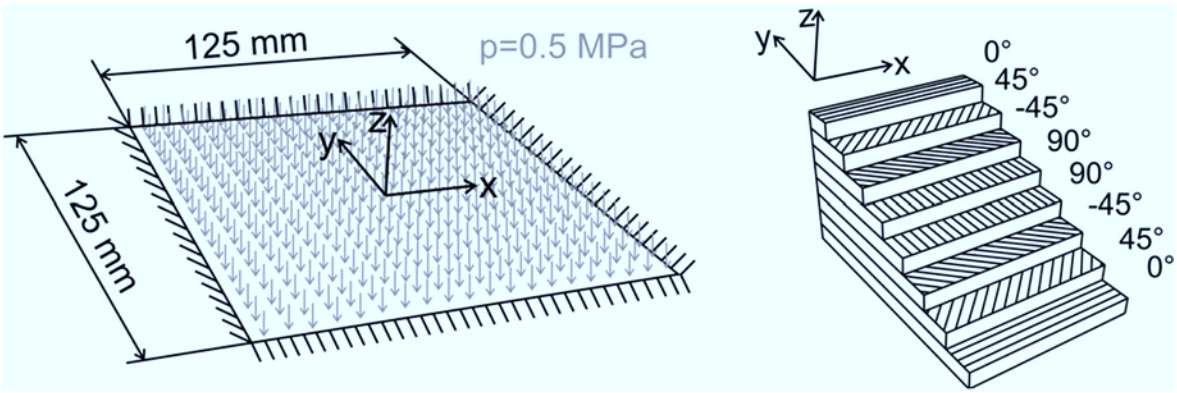

Fig. 4. Force and displacement boundary condition of the analyzed plate and schematic illustration of the LSS $[0, 45, -45, 90]_S$

Material properties, damage parameters, hardening parameters and critical values of damage parameters [2] are given in Tables 1–3. Subscripts t and c in Table 3 denote critical damage parameter values for tensile and compressive loading, respectively. Critical value for damage parameter D_2 is listed only for tensile loading because it is difficult to find accurate model for estimating the critical value of this parameter for transverse compressive loading. In this model it is assumed that critical value of this parameter for compressive loading is equal to critical value for tensile loading. Parameters J_{33} and H_3 are equal to zero. The plate model was divided into 20×20 elements and was analyzed in 50 load substeps.

Table 1. Material properties

	E_1 [GPa]	E_2 [GPa]	G_{12} [GPa]	ν_{12}
M30/949	167	8.13	4.41	0.27
M40/948	228	7.99	4.97	0.292

Table 2. Damage and hardening parameters

	J_1	J_2	H_1	H_2	γ_0	c_1	c_2
M30/949	$0.952 \cdot 10^{-3}$	0.438	$25.585 \cdot 10^{-3}$	$-21.665 \cdot 10^{-3}$	-0.6	0.30	-0.395
M40/948	$2.208 \cdot 10^{-3}$	0.214	$10.503 \cdot 10^{-3}$	$-8.130 \cdot 10^{-3}$	-0.12	0.10	-0.395

Table 3. Critical values of damage variables

	D_{1t}^{cr}	D_{1c}^{cr}	$D_{2t}^{cr} = D_{2c}^{cr}$	k_s
M30/949	0.105	0.111	0.5	0.944
M40/948	0.105	0.111	0.5	0.908

Linear static analysis of the plate with LSS of $[0, 45, -45, 90]_S$ has shown that maximum magnitudes of stresses in fiber direction and direction transverse to fibers as well as equivalent (von Mises) stress occur in the outer layers in the middle of two opposite edges of the plate and maximum magnitudes of shear stress in lamina coordinate system occur in layers 2 (2nd from the bottom) and 7. However, the results of damage analysis have shown that critical damage level will not be reached in the outer layers at first, but in layer 2 (2nd layer from the bottom) and layer 7 for both materials.

For plate from material M30/949 critical damage level has been reached between 17th and 18th load substep in several locations in layer 2 and layer 7. Critical loading for plate from this material (macrocrack will be present in the plate) is $p = 0.175$ MPa. For material M40/948 critical damage level has been reached between 46th and 47th load substeps in several locations in layer 2 and layer 7. Critical loading is $p = 0.465$ MPa. In Figs. 5–6 evolution of stress vs. strain in lamina (local) coordinate system in layer 7 in integration point where critical damage level was reached at first for LSS $[0, 45, -45, 90]_S$ for both materials are shown. In Figs. 7–8 evolution of damage variables in the same point are shown.

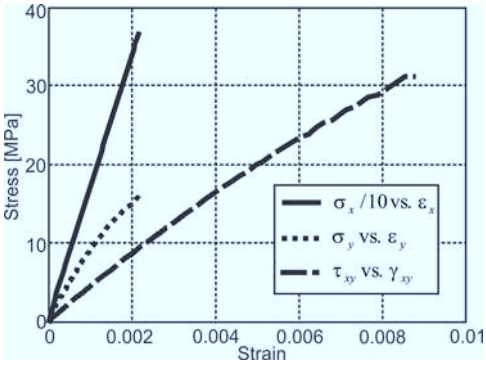

Fig. 5. Stress vs. strain evolution in lamina coordinate system in layer 7 in integration point where critical damage level was reached at first for material M30/949 and LSS $[0, 45, -45, 90]_S$

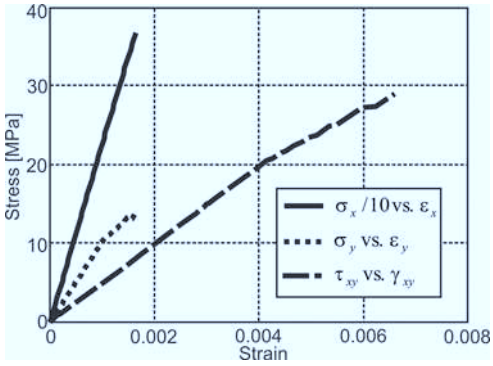

Fig. 6. Stress vs. strain evolution in lamina coordinate system in layer 7 in integration point where critical damage level was reached at first for material M40/948 and LSS $[0, 45, -45, 90]_S$

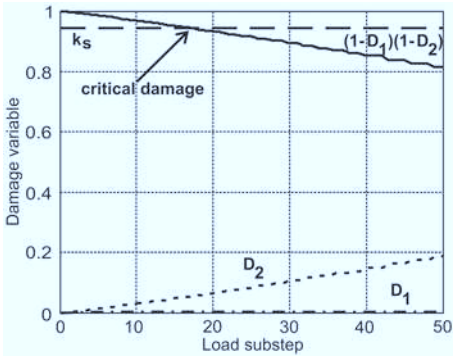

Fig. 7. Evolution of damage variables in layer 7 in integration point where critical damage level was reached at first for material M30/949 and LSS $[0, 45, -45, 90]_S$

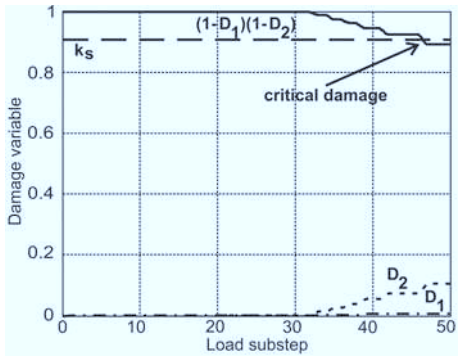

Fig. 8. Evolution of damage variables in layer 7 in integration point where critical damage level was reached at first for material M40/948 and LSS $[0, 45, -45, 90]_S$

Linear static analysis of the plate with LSS of $[0, 90, 45, -45]_S$ has shown that maximum magnitudes of stresses in fiber direction and direction transverse to fibers as well as shear stress in lamina coordinate system and equivalent (von Mises) stress occur in the outer layers. Results of damage analysis have shown that critical damage level for plate from material M30/949 will be reached in these layers. Critical damage level has been reached between 29th and 30th load substep. Critical loading for plate from this material is $p = 0.299$ MPa. For plate from material M40/948 critical damage level has not been reached.

On the other hand linear static analysis of the plate with LSS of $[45, 0, -45, 90]_S$ has shown that maximum magnitudes of stresses in fiber direction and direction transverse to fibers as well as equivalent (von Mises) stress do not occur in the outer layers, but in layers 2 and 7. Maximum magnitudes of shear stress in lamina coordinate system occur in the outer layers. Critical damage level in plate with this LSS will be reached in the outer layers at first for both materials. Critical damage level has been reached between 13th and 14th load substep in plate from material M30/949 and between 34th and 35th load substep in plate from material M40/948. Critical loadings are $p = 0.137$ MPa and $p = 0.346$ MPa.

Overall results of the damage analyses relating to the critical damage level for all LSSs and both materials are listed in Table 4. In Figs. 9–14 distribution of value of the product $(1 - D_1)(1 - D_2)$, which is required for assessing the critical damage level, in layers 1 and 2 for plate from material M30/949 with LSS of $[45, 0, -45, 90]_S$ after applying 15, 30 and 50 load substeps, which corresponds to loadings 0.15 MPa, 0.30 MPa and 0.50 MPa.

Table 4. Overall results of the damage analyses relating to critical damage level

LSS	material	layers in which the critical damage level was reached at first	layers with critical damage level after applying full loading	critical loading
$[0, 45, -45, 90]_S$	M30/949	2, 7	1, 2, 3, 6, 7, 8	0.175 MPa
	M40/948	2, 7	2, 7	0.465 MPa
$[0, 90, 45, -45]_S$	M30/949	1, 8	1, 2, 3, 6, 7, 8	0.299 MPa
	M40/948	–	–	–
$[45, 0, -45, 90]_S$	M30/949	1, 8	1, 2, 3, 6, 7, 8	0.137 MPa
	M40/948	1, 8	1, 8	0.346 MPa

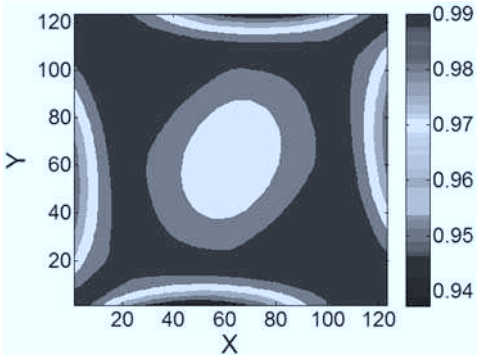

Fig. 9. Distribution of the value of $(1 - D_1)(1 - D_2)$ in layer 1, material M30/949, LSS $[45, 0, -45, 90]_S$ after load substep 15 ($p = 0.15$ MPa)

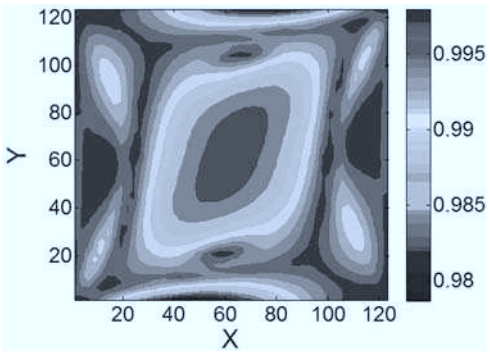

Fig. 10. Distribution of the value of $(1 - D_1)(1 - D_2)$ in layer 2, material M30/949, LSS $[45, 0, -45, 90]_S$ after load substep 15 ($p = 0.15$ MPa)

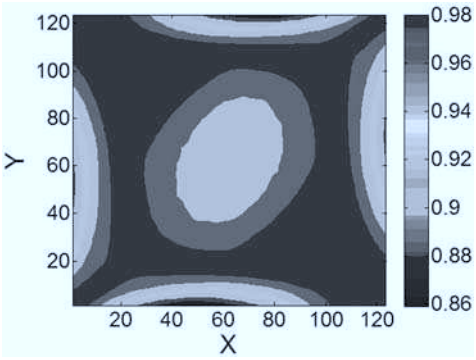

Fig. 11. Distribution of the value of $(1 - D_1)(1 - D_2)$ in layer 1, material M30/949, LSS $[45, 0, -45, 90]_S$ after load substep 30 ($p = 0.30$ MPa)

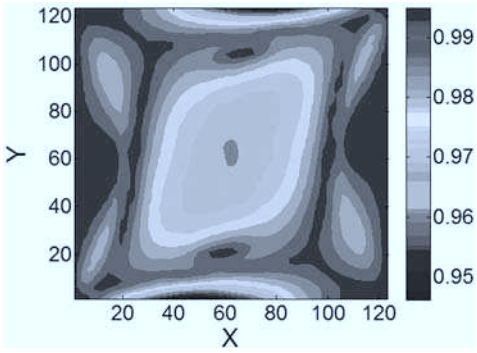

Fig. 12. Distribution of the value of $(1 - D_1)(1 - D_2)$ in layer 2, material M30/949, LSS $[45, 0, -45, 90]_S$ after load substep 30 ($p = 0.30$ MPa)

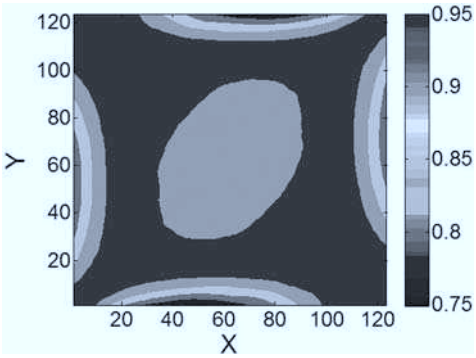

Fig. 13. Distribution of the value of $(1 - D_1)(1 - D_2)$ in layer 1, material M30/949, LSS $[45, 0, -45, 90]_S$ after load substep 50 ($p = 0.50$ MPa)

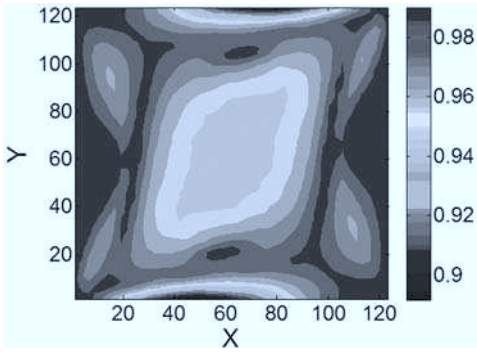

Fig. 14. Distribution of the value of $(1 - D_1)(1 - D_2)$ in layer 2, material M30/949, LSS $[45, 0, -45, 90]_S$ after load substep 50 ($p = 0.50$ MPa)

5. Conclusion

In the current study, we have focused on solving elastic damage analysis of thin laminated long fiber-reinforced composite plate consisting of unidirectional layers which is fixed on its edges and loaded by uniformly distributed pressure for different materials and different LSSs. The postulated damage surface reduces to the Tsai-Wu surface in stress space. However, presented model goes far beyond simple failure criteria by identifying a damage threshold, hardening parameters for the evolution of damage, and critical values of damage for which material failure occurs. The analysis results show that change of material, change of laminate stacking sequence as well as presence of shear stress have significant influence on the evolution of damage as well as on location of critical damage and load at which critical level of damage will be reached. Critical damage level has not necessary to be reached in places with maximum magnitude of equivalent stress, but can be reached in other places.

Acknowledgements

The authors gratefully acknowledge the support by the Slovak Grant Agency VEGA 09-015-00 and VEGA 1/1226/12

References

[1] Bathe, K. J., Finite Element Procedures, Prentice Hall, New Jersey, 1996.

[2] Barbero, E. J., de Vivo, L., A Constitutive Model for Elastic Damage in Fiber-Reinforced PMC Laminae. International Journal of Damage Mechanics 10 (1) (2001) 73–93.

[3] Barbero, E. J., Finite Element Analysis of Composite Materials, CRC Press, Boca Raton, 2007.

[4] Chen, Y., Lee, J. D., Eskandarian, A., Meshless Methods in Solid Mechanics, Springer, New York, 2006.

[5] Guiamatsia, I., Falzon, B. G., Davies, G. A. O., Iannucci, L., Element-free Galerkin modelling of composite damage, Composites Science and Technology 69 (2009) 2 640–2 648.

[6] Jain, J. R., Ghosh, S., Damage Evolution in Composites with a Homogenization-based Continuum Damage Mechanics Model, International Journal of Damage Mechanics 18 (6) (2009) 533–568.

[7] Jirásek, M., Zeman, J., Deformation and damage of materials, Czech Technical University, Prague, 2006. (in Czech)

[8] Kaw, A. K., Mechanics of Composite Materials. 2nd ed., CRC Press, Boca Raton, 2006.

[9] Kollár, L., Springer, G. S., Mechanics of Composite Structures, Cambridge University Press, New York, 2003.

[10] Kompiš, V., Žmindák, M., Kaukič, M., Computational methods in mechanics: Linear analysis, University of Žilina, Žilina, 1997.

[11] Kormaníková, E., Riecky, D., Žmindák, M., Strength of composites with fibers, In Murín, J., Kompiš, V., Kutiš, V., eds.: Computational Modelling and Advanced Simulations, Springer Science + Business Media B.V., 2011.

[12] Laš, V., Zemčík, R., Progressive Damage of Unidirectional Composite Panels, Journal of Composite Materials 42 (1) (2008) 25–44.

[13] Liu, G. R., Gu, Y. T., An Introduction to Meshfree Methods and Their Programming, Springer, Berlin, 2005.

[14] Puck, A., Schurmann, H., Failure analysis of FRP laminates by means of physically based phenomenological models, Composite Science and Technology 62 (12–13) (2002) 1 633–1 662.

[15] Tay, T. E., Liu, G., Yudhanto, A., Tan, V. B. C., A Micro Macro Approach to Modeling Progressive Damage in Composite Structures, International Journal of Damage Mechanics 17 (1) (2008) 5–28.

[16] Tumino, D., Capello, F., Catalanotti, G., A continuum damage model to simulate failure in composite plates under uniaxial compression, Express Polymer Letters 1 (1) (2007) 15–23.

[17] Ventsel, E., Krauthammer, T., Thin Plates and Shells: Theory, Analysis, and Applications, Marcel Dekker, Inc., New York, 2001.

[18] Voyiadjis, G. Z., Kattan, P. I., A Comparative Study of Damage Variables in Continuum Damage Mechanics, International Journal of Damage mechanics 18 (4) (2009) 315–340.

[19] Zhang, Y. X, Chang, C. H., Recent developments in finite element analysis for laminated composite plates, Composite Structures 88 (1) (2009) 147–157.